THERMAL FIELD AROUND A CIRCULAR CYLINDER WITH PERIODIC VORTEX SHEDDING

M. Molki and D. Fotouhi

Department of Mechanical Engineering
Isfahan University of Technology
Isfahan, Iran

Abstract A numerical study is carried out to investigate the laminar forced convection heat transfer from a circular cylinder. The fluid is assumed to be incompressible, the Reynolds number ranged from 0.1 to 1000, and the Prandtl number was equal to 0.7. The range of study includes heat transfer in creeping flow (Re<1), flow with steady and symmetric eddies (7≤Re≤40), and the flow with periodic vortex shedding (Re>40). The equations were discretized by a control-volume-based finite difference technique, and they were solved by the SIMPLE algorithm. The problem formulation is such that it can handle both steady and steady periodic situations. The paper presents the isotherms for the cylinder with isothermal wall and constant wall heat flux. The results indicate that the periodic nature of eddies causes an oscillatory behavior in the heat transfer coefficients. The oscillations are intensified as the Reynolds number is increased.

Key Words Cylinder, Heat Transfer, Vortex Shedding, Laminar Flow, Forced Convection

چکیده انتقال حرارت در جریان آرام در اطراف استوانه به روش عددی بررسی شده است. سیال تراکم ناپذیر بوده و تغییرات عدد رینولدز از ۰/۱ تا ۱۰۰۰ و عدد پرانتل برابر با ۰/۷ است. گسترهٔ این بررسی به گونه ای است که انتقال حرارت در جریان خزشی (Re <۱)، جریان توأم با گردابه های متقارن در حالت دائم (۷ ≤ Re ≤۴۰) و جریان همراه با گردابه های تناوبی (Re > ۴۰) را شامل می شود. معادلات به روش تفاضل محدود مبتنی بر حجم معیار به صورت گسسته درآمده و با الگوریتم سیمپل حل شده است. فرمولبندی مسئله می تواند شرایط دائم و دائم تناوبی را درنظر بگیرد. دراین مقاله خطوط تکدما برای استوانهٔ با دمای ثابت و استوانهٔ با شار حرارتی ثابت ارائه شده است. نتایج نشان می دهد که ضریب انتقال حرارت دراثر تناوب گردابه ها نوسان می کند. این نوسانها با افزایش عدد رینولدز تقویت می شوند.

INTRODUCTION

The flow of fluid around cylinders is diverse and complex. The special features of the flow depends on the value of Reynolds number. For Re <1, the flow is identified as creeping flow, and the Oseen [1] solution can be used. In this case, the fluid flows smoothly around the cylinder and there is no evidence of eddy or recirculating motion behind the cylinder. The formation of the first eddies is observed when Re is near 7 [2]. The eddies are symmetric and stable. However, as Re is increased, the eddies become longer.

The complexity of the flow becomes apparent when Re exceeds 40. The eddies behind the cylinder begin to oscillate. They are periodically separated from the cylinder and are released in the flow. The oscillatory motion of the flow increases with Re. These oscillations are mainly limited to the region behind the cylinder and affect the local parameters of the fluid there. The complex recirculating flow has profound effect on heat transfer. For example, one can refer to the strong oscillations of heat transfer coefficient at high Re.

Heat transfer in flow around cylinders has been the subject of many previous investigations [4-17]. Some investigators have studies the effect of buoyancy [18] and some others have focused on the accuracy of numerical techniques and bench marking them for the flow around cylinders [19]. Despite the

aforementioned studies, it appears that the effect of oscillating eddies and their oscillatory effect on heat transfer coefficient has not been paid the due attention before.

This article considers the effect of eddy motion on heat transfer in the range $0.1 \leq Re \leq 1000$. The computations are carried out for constant wall temperature and constant heat flux. The prandtl number is fixed at 0.7, corresponding to that for air. The problem is solved by a well-known numerical method [3]. The results presented in this paper are isothermal contours, temporal and spatial variation of heat transfer coefficients, and heat transfer coefficients at the stagnation point. The flow is entirely assumed to be laminar. The problem of transition to turbulence is discussed in [20].

FORMULATION OF THE PROBLEM

The flow behavior can be formulated mathematically by writing the governing differential equations. The appropriate equations are: continuity, momentum, and energy equations which have to be written in cylindrical coordinates. In terms of dimensionless parameters, the equations are,

Continuity

$$\frac{\partial}{\partial R}(RV) + \frac{\partial U}{\partial \theta} = 0 \qquad (1)$$

Radial component of momentum

$$\frac{\partial V}{\partial t} + V\frac{\partial V}{\partial R} + \frac{U}{R}\frac{\partial V}{\partial \theta} = -\frac{\partial P}{\partial R} + \frac{2}{Re}\nabla^2 V + \frac{U^2}{R} - \frac{2}{Re}\left(\frac{V}{R^2} + \frac{2}{R^2}\frac{\partial U}{\partial \theta}\right) \qquad (2)$$

Angular component of momentum

$$\frac{\partial U}{\partial t} + V\frac{\partial V}{\partial R} + \frac{U}{R}\frac{\partial U}{\partial \theta} = -\frac{1}{R}\frac{\partial P}{\partial \theta} + \frac{2}{Re}\nabla^2 U - \frac{UV}{R} + \frac{2}{Re}\left(\frac{2}{R^2}\frac{\partial V}{\partial \theta} - \frac{U^2}{R}\right) \qquad (3)$$

Energy

$$\frac{\partial T}{\partial t} + V\frac{\partial T}{\partial R} + \frac{U}{R}\frac{\partial T}{\partial \theta} = \frac{2}{Re.Pr}\nabla^2 T \qquad (4)$$

The initial condition for velocity is the same as that in the inviscid flow around the cylinder, except for the velocities on the wall which are equal to zero. The initial temperature is equal to the temperature of the free stream fluid (T=0). The boundary conditions are zero velocities on the surface of the cylinder and uniform velocity far upstream from the cylinder. Two thermal boundary conditions were considered: constant wall temperature T_w and constant wall heat flux q_w. Temperature of the distant fluid is uniform and equal to zero. In Equations 1 to 4, the fluid properties are assumed to be constant. Thus, the momentum equations are decoupled from the energy equation. In the present computations, in each time step, Equations 1 to 3 were solved first. The obtained velocity field was then fed into the energy equation to get the temperature field.

COMPUTATIONAL APPROACH

The above equations were discretized by a control-volume-based finite difference method and solved numerically by the SIMPLE algorithm. The computational mesh used in this work is shown in Figure 1. The cylinder is positioned at the center of the mesh, as can be seen as a white circular point at the center. The mesh was generated algebraically in such a way that to cluster the grid points near the cylinder. The upstream half of the mesh had fewer points in the peripheral direction, while the downstream half was denser. This arrangement could give better resolution near the cylinder wall and in the

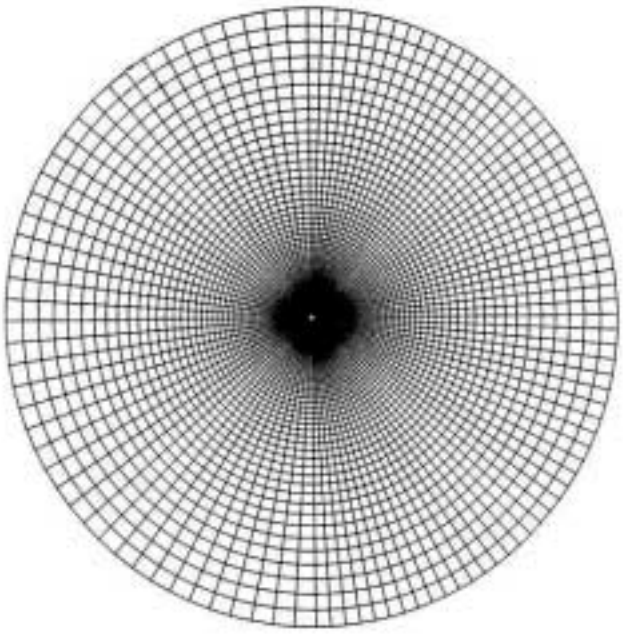

Figure 1. The computational mesh. Flow is from left to right.

downstream area where vortices were present.

The conservation equations mentioned earlier may be cast into the following general form,

$$\partial(\rho\phi)/\partial t + div(\rho\vec{u}\phi) = \text{div}\,(\Gamma\ \text{grad}\ \phi) + S_\phi \qquad (5)$$

where the source term S_ϕ for V and U velocity components are,

$$S_V = U^2/R - (2/Re)\,[V/R^2 + 2/R^2(\partial U/\partial\theta)] - \partial P/\partial R \qquad (6)$$

$$S_U = -UV/R + (2/Re)[(2/R^2)(\partial V/\partial\theta) - U/R^2] - 1/R(\partial P/\partial\theta) \qquad (7)$$

These source terms were linearized and used in the discretization equations. Details of the linearization method is outlined in [3].

The time integration of various terms of the differential equations was carried out by fully implicit method and the interface values were interpolated by power-law [3]. The continuity equation was applied implicitly via a pressure correction equation. In every time step, the computations of the momentum equations were continued until the velocity field converged. The velocity results were subsequently fed into Equation 4 and the computations proceeded to convergence.

The outer boundary of the computational mesh (large outer circle in Figure 1) was positioned at 103 radii from the cylinder axis. Before the onset of the final computations, extensive numerical experiments were performed to determine the location of the outer boundary, number of mesh points, time increment, and convergence criterion. A sample of grid study is outlined in Tables 1 to 4. In these tables the effect of number of grid points, location of the outer boundary, mass residual appearing in the pressure correction equation [3], and time step on important parameters has been investigated. From these initial runs, it was decided to have the outer boundary at 103 radii from the cylinder axis, 9240 mesh points, a time increment of 0.02, and the maximum mass residual (used as the convergence criterion) of 10^{-6}. All computations were performed on a 486

TABLE 1. Grid Study (Re=100).

Grid Points	Drag coefficient, C_D	Separation angle, degree	Mean Nu	Nu at stagnation point, Nu_s
5084	1.161	110.21	5.335	10.200
9020	1.172	111.35	5.216	9.751
11408	1.179	112.10	5.182	9.640

TABLE 2. Effect of the Outer Boundary (Re=100).

Boundary location, R	Separation angle, degree	Mean Nu	Nu at stagnation point, Nu_s
28.8	110.68	5.312	9.833
91.2	110.89	5.283	9.775
191.3	110.90	5.270	9.747

DX2 (66 MHz) personal computer. The typical CPU times for the runs are shown in Tables 3 and 4. These values are for the runs that started from the initial condition and continued to t=30. However, since the final computations were continued to t=150, the CPU times in these tables should be multiplied by (150/30=) 5 to find CPU time for the final runs.

RESULTS AND DISCUSSION

The isotherms for the cylinder with constant wall temperature are presented in Figure 2a. The flow is from left to right and the numbers in the figure refer to the time sequence. The isotherms are plotted for a large time in which the initial transients have damped out and the steady periodic state has been established. In this state, the eddies oscillate behind the cylinder and distort the isotherms. The high density of the isotherms in front of the cylinder indicates a large temperature gradient there. It is noteworthy that the propagation of thermal field in front of the cylinder is limited to a thin layer of fluid there. In contrast, the major thermal influence is observed behind the cylinder where the thermal effects travel to far distances downstream. Another view of the thermal wakes can be seen in Figure 2b. These photographs correspond to the isotherms of Figure 2a identified with numbers 3 and 5. The regions of uniform color represent the nearly isothermal bands.

Figure 3 presents the isotherms for the cylinder

TABLE 3. Effect of Mass Residual (Re=100, Grid points=9020, t=30).

Mass residual	Separation angle, degree	Mean Nu	Nu at stagnation point, Nu_s	CPU time, hr: min: sec
10^{-5}	110.79	5.28537	9.77626	04:03:23
10^{-6}	110.88	5.28301	9.77475	12:57:32
10^{-7}	110.89	5.28295	9.77473	40:30:26
10^{-9}	110.89	5.28295	9.77472	65:02:50

TABLE 4. Effect of Time Step (Re=100, Grid points=9020, t=30).

Time step Δt	Separation angle, degree	Mean Nu	Nu at stagnation point, Nu_s	CPU time, hr: min: sec
0.2	110.91	5.28339	9.77461	19:07:39
0.1	110.89	5.28295	9.77473	40:30:26
0.02	110.82	5.28296	9.77597	82:51:42
0.01	110.82	5.28290	9.77602	Not available

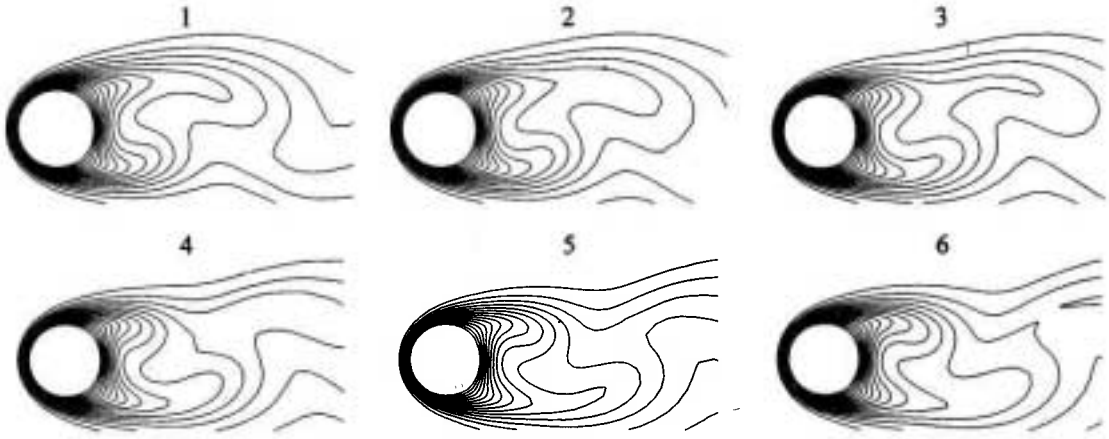

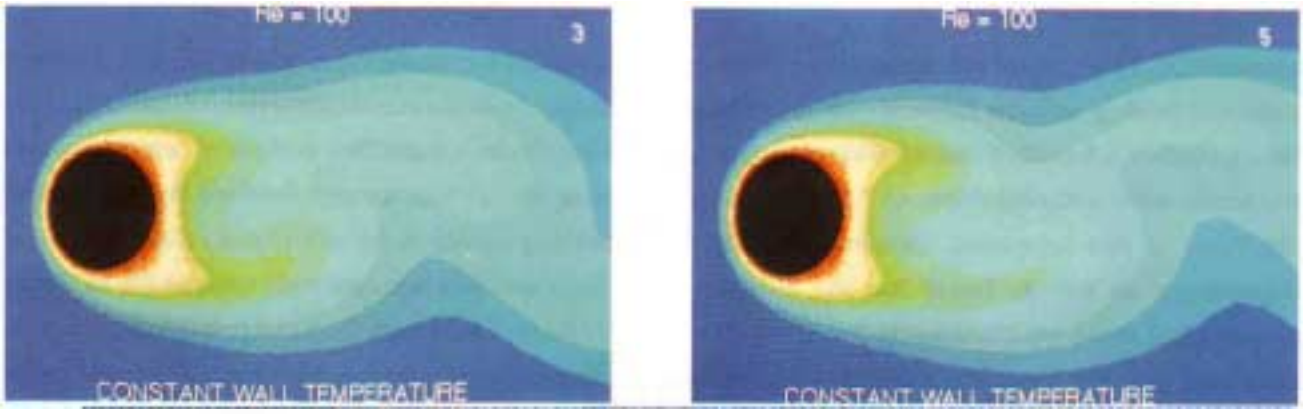

Figure 2 .(a) Isotherms for the cylinder with constant wall temperature, Re = 100. The numbers in the diagrams refer to the time sequence. **(b)** Photographs of the isotherms for the cylinder with constant wall temperature, Re =100. Numbers 3 and 5 in the upper right corner refer to the same numbers in Figure 2a.

with constant heat flux. In this case, the wall temperature is not constant and the isotherms , as can be seen in the figure, intersect with the cylinder surface. Despite this point, the thermal field seen in Figures 2a and 3 are not very different.

Temporal variation of heat transfer coefficient and its approach to the steady periodic state are shown in Figure 4. At low Re, the eddies behind the cylinder are stable and there is no evidence of oscillation in heat transfer coefficient. However, as Re is increased the eddies and heat transfer coefficients begin to oscillate. As seen in the figure, the oscillations are intensified with increase in Re.

A more useful result for practical engineer is the mean heat transfer coefficient. In Figure 5, the mean Nusselt number $\overline{Nu}$ is plotted against Re and is compared with those in the literature. The figure shows that heat transfer coefficient increases with Re. If Re is restricted to a narrow range, the variations can be well represented by $\overline{Nu} = a\,Re^{b}Pr^{c}$. However, since the present investigation covers a large range of Re, this is not possible.

A careful attention to the data obtained in the present work shows that heat transfer coefficient for constant heat flux condition (open circles in Figure 5) is always higher than that for the constant wall

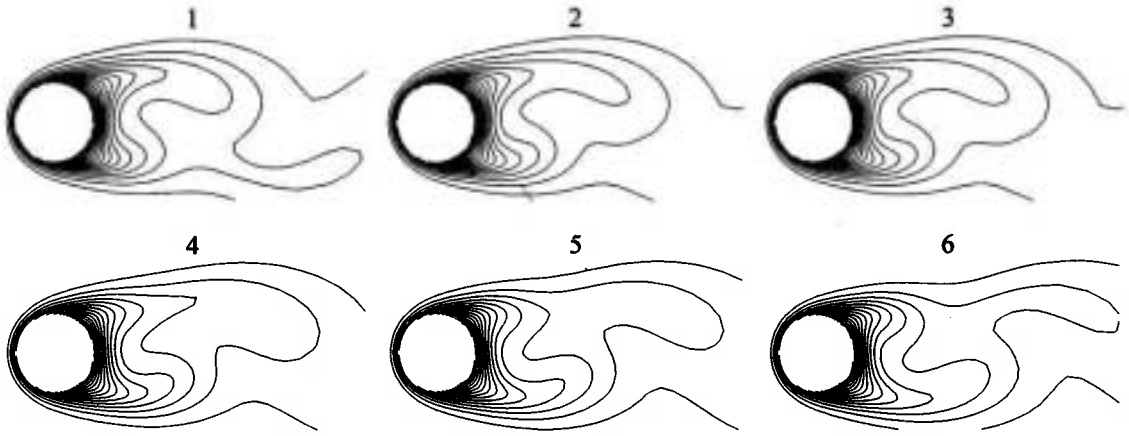

Figure 3. Isotherms for the cylinder with constant wall flux, Re = 100. The numbers in the diagrams refer to the time sequence.

temperature. This is observed in many heat transfer problems dealing with the boundary layer or shear layers. Further, it is noticed that at lower values of Re, the results show a smaller slope. As Re is increased, the slope is also increased, showing a stronger dependence on Re. At lower Re, the diffusion (conduction) terms are dominant in the differential equations, and the Nusselt number is expected to approach a constant value. Indeed, if Re approaches zero and a stagnant cylindrical body of fluid envelopes the cylinder, a simplified analysis of heat conduction from the cylinder through the fluid layer under this limiting condition would lead to a value of 0.432 for Nu. This value is surprisingly close to Nu values of 0.501 (constant heat flux) and 0.489 (constant wall temperature) for the two data points corresponding to Re=0.1 in Figure 5. This limiting-case comparison together with the good agreement seen with other investigations in the figure, supports the present computational approach.

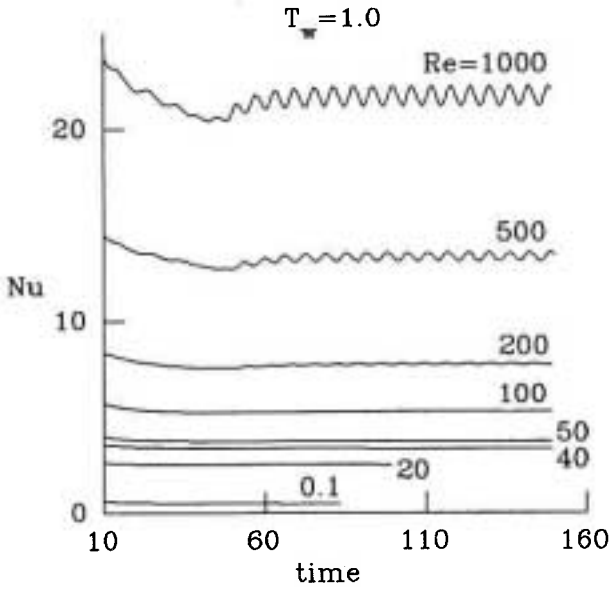

Figure 4. Temporal variation of heat transfer coefficient for the cylinder with constant wall temperature. At higher Re, the heat transfer coefficient oscillates in time.

Local heat transfer coefficients at a specific time are presented in Figure 6. The angle θ=0 in this figure corresponds to the stagnaion point in front of the cylinder. The largest heat transfer coefficient occurs at this point. As θ is increased, the heat transfer coefficient decreases rapidly due to the growth of the boundary layer. The coefficient attains its minimum value at the point of separation, thereafter it increases due to high flow activities in the wake region behind the cylinder. The flow activities are strengthened as Re is increased and the corresponding graphs indicate higher increases.

It should be noted that as Re is increased to 40,

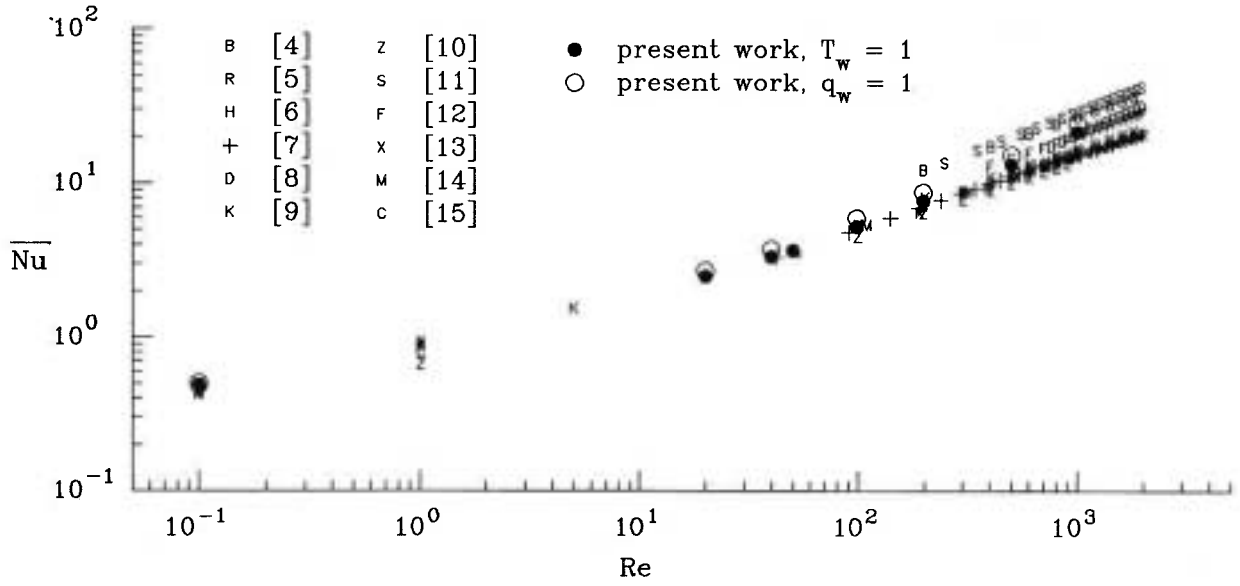

Figure 5. Mean Nusselt number and comparison with the literature.

periodic vortex shedding is observed downstream. The periodic character of the vortices affect the separation point, so that the point of separation also oscillates with time. So, it may be concluded that separation angle is a function of both Re and time. The asymmetry seen in Figure 6 at Re> 40 is a reflection of these oscillations. If Nu_θ curves are plotted for a specific value of Re>40 at different times, the curves would not be coincident.

Figure 7 presents similar results for the constant heat flux condition. The general trend is similar to Figure 6. However, the variations of the heat transfer

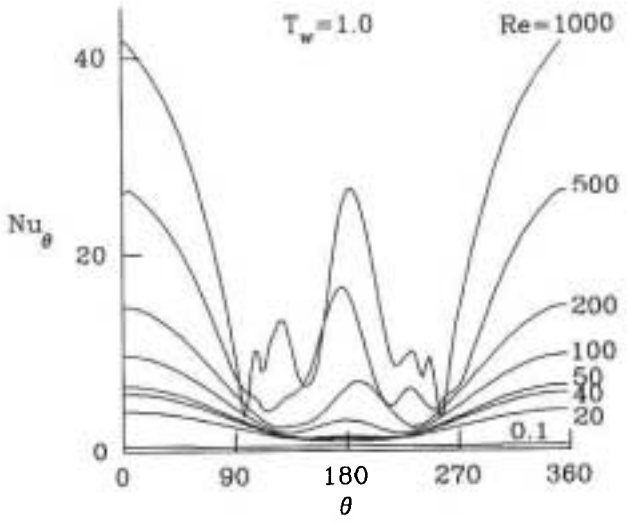

Figure 6. Local heat transfer coefficient for the cylinder with constant wall temperature . The graphs are not symmetric due to the eddy oscillations.

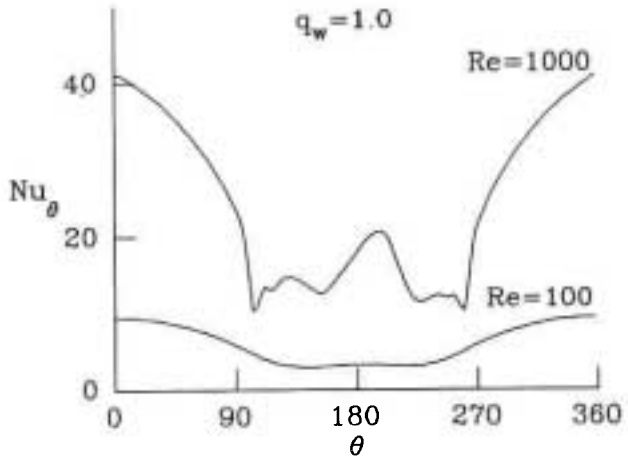

Figure 7. Local heat transfer coefficient for the cylinder with constant wall heat flux. The graphs are not symmetric due to the eddy oscillations.

coefficient in the wake region is less pronounced.

For the cylinder with constant heat flux, the surface temperature is variable. Surface variation for Re=100 and 1000 is presented in Figure 8. The boundary layer thickness and thermal resistance increase with θ. Therefore, to keep the heat flux constant, the surface temperature should increase. This tempearture increase is clearly seen in Figure 8. It is noteworthy that the flow separation further downstream disturbs the boundary layer and prevents further increase in temperature. Figure 8 shows that after the point of separation, the surface temperature decreases slightly. The temperature fluctuations seen in this region are due to the oscillation of the eddies behind the cylinder.

For the cylinder with a constant wall temperature, the wall heat flux is a function of θ (Figure 9). The largest value of heat flux occurs at the stagnation point (θ = 0) and the lowest value is at the point of separation. In the wake region, depending on Re, the heat flux may remain constant or fluctuate with time. The flow activities in the wake region are intensified with Re, and the fluctuations of heat flux are increased.

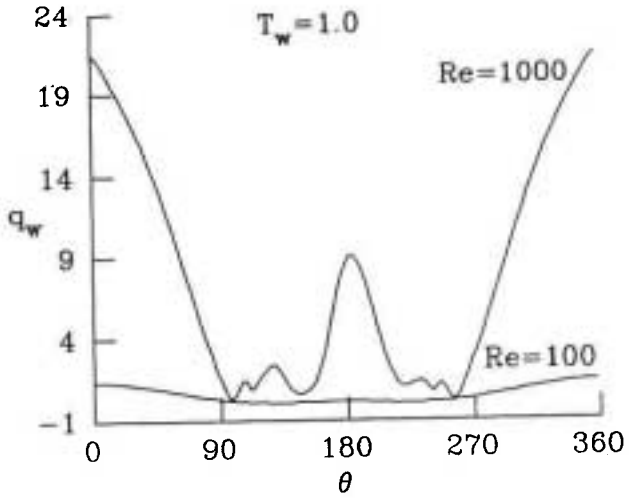

Figure 9. Variation of the wall heat flux for the isothermal cylinder. The largest heat flux occurs at the stagnation point.

The heat transfer coefficient for the stagnation point for the two thermal boundary conditions is presented in Figure 10. The heat transfer coefficient increases with Re. As can be seen from the figure, the type of boundary condition is apparently insignificant

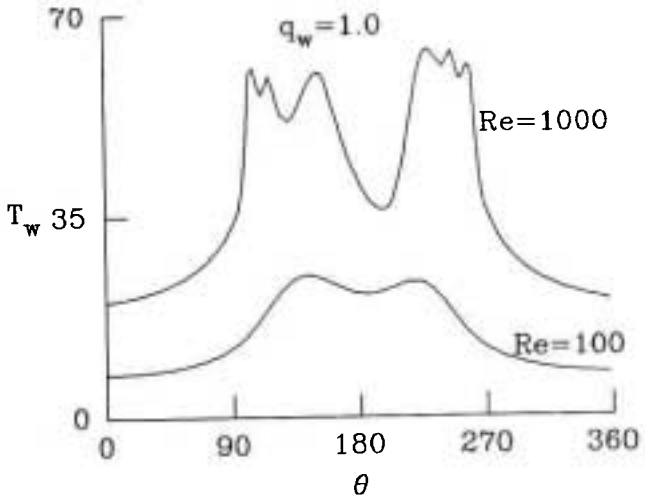

Figure 8. Variation of the wall temperature for the cylinder with constant heat flux. The hot spot is near the point of separation where the boundary layer is thick.

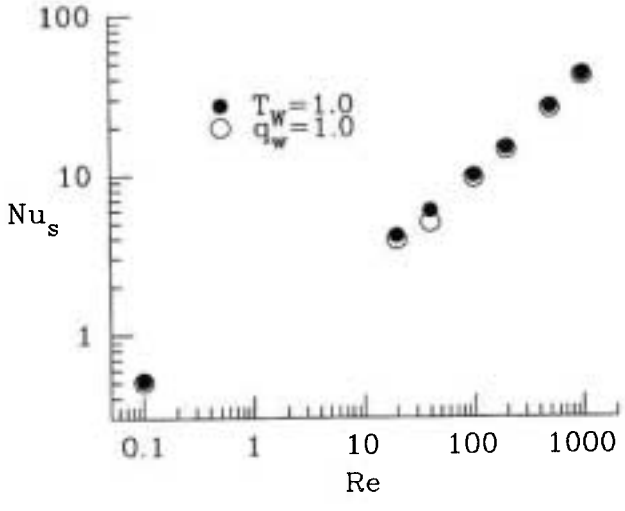

Figure 10. Heat transfer coefficient at the stagnation point. The effect of the thermal boundary condition on heat transfer coefficient is apparently insignificant.

and the data points for the two condition are nearly overlapped. It should be noted, however, that in most heat transfer problems, the Nusselt number for constant heat flux condition is generally higher than that for the constant wall temperature. Apparently this does not apply to the stagnation point of the cylinder, as evidenced from Figure 10.

CONCLUDING REMARKS

In this article, a numerical investigation was performed to study heat transfer for laminar incompressible flow around cylinder. The eddies formed behind the cylinder affect the thermal fiels. For Re > 40, the eddies oscillate and cause oscillations of the isotherms. The temperature variations in front of the cylinder is restricted to boundary layer and does not influence the upstream fluid. Behind the cylinder, however, the formation of eddies and release of them in the flow causes the thermal wakes to travel to far distances downstream. The results for the two thermal boundary conditions indicate that the heat transfer coefficients are nearly insensitive to the boundary conditions. The heat transfer coefficients oscillate at higher Re, and the oscillations are strengthened as Re is increased. The largest heat transfer coefficient occurs at the stagnation point and the lowest value is at the point of separation. Depending on the Re value, the heat transfer coefficient behind the cylinder is either constant or oscillatory.

NOMENCLATURE

c	specific heat
h	convective heat transfer coefficient
h_θ	local heat transfer coefficient at θ location
h_s	local heat transfer coefficient at stagnation point (θ = 0)
k	thermal conductivity of the fluid
Nu	Nusselt number, h(2R)/k
$\overline{Nu}$	mean Nusselt number $(\int_0^{2\pi} Nu_\theta d\theta)/2\pi$
Nu_θ	local Nusselt number, $h_\theta(2R)/k$
Nu_{max}	maximum values of fluctuating Nusselt number in Nu graphs (Figure 4)
Nu_{min}	minimum values of fluctuating number in Nu graphs (Figure 4)
Nu_s	Nusselt number at stagnation point
p	fluid pressure
P	dimensionless fluid pressure, $p/\rho u_\infty^2$
Pr	Prandtl number, ν/α
q_w	wall dimensionless heat flux, $q'_w/(\rho c u_\infty \Delta T')$
q'_w	wall heat flux
r	radial coordinate, r = 0 refers to the center of the cyliner
R	dimensionless radial coordinate, r/R cylinder radius
Re	Reynolds number, $u_\infty(2R)/n$
t	dimensionless time, $\tau u_\infty/R$
T	$(T'- T'_\infty)/(T'_s-T'_\infty)$
T_w	wall temperature
T′	temperature
T'_s	temperature at the stagnation point
T'_∞	free stream temperature
u	circumferential velocity component
U	dimensionless circumferential velocity component, u/u_∞
u_∞	free stream velocity
v	radial velocity component
V	dimensionless radial velocity component, v/u_∞

Greek Symbols

α	thermal diffusivity, k/ρc
ΔT′	$(T'_s - T'_\infty)$
θ	circumferential coordinate, θ = 0 at stagnation point in front of the cylinder
μ	fluid viscosity
ν	kinematic viscosity, μ/ρ
ρ	fluid density
τ	time
∇^2	Laplacian operator

REFERENCES

1. F. M. White, "Viscous Fluid Flow," 2nd edition, McGraw-Hill, New York (1991).
2. S. C. R. Dennis and Gau-Zu Chang, "Numerical Solution for Steady Flow Past a Circular Cylinder at Reynolds Numbers up to 100", *J. Fluid Mechanics*, Vol. 42, (1970), 471-489.
3. S. V. Patankar, "Numerical Heat Transfer and Fluid Flow," Hemisphere, Wash. (1980).
4. J. Boussinesq, "Mise en Equation des Phenomenes de Convection Calorifique et Apercu sur le Pouvoir Refroidissant des Fluides," *C. R. Acad. Sci.*, Vol. 132, (1901), 1382-1387.
5. C. W. Rice, "Free and Forced Convection of Heat in Gases and Liquids, "*Trans. AIEE*, Vol., 42 (1923), 653-701.
6. R. Hilpert, *Forsch. Geb. Ingenieurwes.*, Vol. 4, (1933), 215.
7. W. H. McAdams, "Heat Transmission," McGraw-Hill, New York (1954).
8. R. J. Dahlen, "A Relation Between Heat and Mass Transfer Coefficients Verified for Adiabatic Evaporation from a Cylinder," Ph.D. Thesis, Purdue Univ., Lafayette, Indiana, (1962).
9. S. S. Kutateladze, "Fundamentals of Heat Transfer," Arnold, London, (1963).
10. A. Zhukauskas, " Heat Transfer from Tubes in Cross Flow," in J. P. Hartnett and T. F. Irvine, Jr., Eds., Advances in Heat Transfer, Vol. 8, Academic Press, New York (1972).
11. H. Saito and K. Kishinami, " Analogy Between Heat and Mass Transfer in Tube Banks," Heat Transfer--Jap. Res., Vol. 1, (1972), 96-103.
12. R. M. Fand and K. K. Keswani, "A Continuous Correlation Equation for Heat Transfer from Cylinders to Air in Crossflow for Reynolds Numbers from 10^{-2} to 2×10^{5}, *Int. J. Heat Mass Transfer*, Vol. 15, (1972), 559-562.